

# A survey of the 6.7 GHz methanol maser emission from IRAS sources

## II. Statistical analysis

M. Szymczak and A.J. Kus

Toruń Centre for Astronomy, Nicolaus Copernicus University, ul. Gagarina 11, 87100 Toruń, Poland

Received 9 May 2000 / Accepted 30 May 2000

**Abstract.** We present an analysis of the 6.7 GHz methanol maser data taken with the 32 m Toruń telescope during recently completed survey of IRAS based sample of star formation sites. Methanol masers are associated with 13% of the sources in the sample. The mean detection rate slightly increases with the IRAS flux density quality measurements. It is 62% for sources with the 60  $\mu\text{m}$  flux density,  $F_{60} > 10^4$  Jy and decreases to 7% for sources with  $F_{60} < 250$  Jy. The detection rate in the inner Galaxy region of 18% is a factor of eight higher than that in the anticentre region. The maser velocity range,  $\Delta V < 6 \text{ km s}^{-1}$  is observed in sources with the mean linewidth,  $\langle \text{FWHM} \rangle \leq 0.14 \text{ km s}^{-1}$ , whereas the distribution of  $\Delta V$  in sources with  $\langle \text{FWHM} \rangle > 0.14 \text{ km s}^{-1}$  is flat with only a slight excess of the source number with  $\Delta V > 10 \text{ km s}^{-1}$ .  $\Delta V$  slightly increases with the [25 – 12] colour and  $\Delta V > 8 \text{ km s}^{-1}$  is usually not observed among the bluest sources ([25 – 12] < 0.5).

Several of the methanol sources found have colours well outside the colour ranges commonly accepted for ultracompact HII regions. The maximum detection rate of methanol masers is observed for specific colour ranges. The maser flux density is weakly correlated with the 60  $\mu\text{m}$  flux density and far-infrared pumping with an efficiency of about 3% is possible. The median photon luminosity of methanol masers in the solar neighbourhood is  $2 \cdot 10^{43} \text{ s}^{-1}$ , being between the OH and H<sub>2</sub>O maser luminosities. The inferred lower limit for the linewidth of  $0.05 \text{ km s}^{-1}$  implies the kinetic temperature of less than 35 K in the methanol maser regions. It is proposed that the differences in the observed maser properties primarily reflect evolutionary changes of star-forming regions.

**Key words:** masers – surveys – stars: formation – ISM: molecules – radio lines: ISM – ISM: H II regions

### 1. Introduction

The 6.7 GHz methanol maser line has been recognized as one of the most prominent phenomena related to the recent or ongoing massive star formation (Menten 1991; Walsh et al. 1998). The high peak luminosity up to  $10^{5-6} \text{ Jy kpc}^2$  in this line (Caswell et

al. 1995) makes it possible to observe the star formation sites to large distances in our Galaxy and strong methanol sources can be mapped with high angular resolution (Walsh et al. 1998). An efficient detection of the 6.7 GHz methanol masers was made towards known interstellar OH sources (Menten 1991; MacLeod et al. 1992; MacLeod & Gaylard 1992; Caswell et al. 1995). Observations of IRAS sources with colours characteristic for ultracompact HII regions (Schutte et al. 1993; van der Walt et al. 1995; 1996; Walsh et al. 1997; MacLeod et al. 1998; Slysh et al. 1999) and blind surveys of selected parts of the galactic plane (Caswell 1996; Ellingsen et al. 1996) resulted in several detections.

With the exception of studies by Menten (1991) and Slysh et al. (1999), other observations have been done in the southern hemisphere. However, to understand the physical properties of the interstellar medium in which stars are born, it is useful to obtain the CH<sub>3</sub>OH maser population as completely as possible. This was one of our objectives to make a comprehensive search for methanol masers in the northern hemisphere. Recently, we reported the observations of IRAS sources where 182 masers were found (Szymczak et al. 2000). In the present paper we deal with the statistical analysis of this data set. Our main aims are (1) to clarify relationships in the observed properties between far-infrared sources and methanol masers, (2) to determine basic parameters of the 6.7 GHz maser line in order to constrain current maser models.

### 2. The sample

The sample of 1399 objects surveyed in the 6.7 GHz methanol line was drawn from the IRAS Point Source Catalog (1985). All the sources have the flux densities at 60  $\mu\text{m}$  larger than 100 Jy, the ratio of the flux densities at 60 and 25  $\mu\text{m}$  is higher than the unity and  $\delta > -20^\circ$ . No requirements for the flux measurement qualities of all four IRAS bands were made. Within these criteria of selection this sample is complete. Further inspection of our sample revealed that 79% of objects satisfy  $F_{12} < F_{25} < F_{60} < F_{100}$ , where  $F_{\lambda_i}$  is the IRAS flux density at wavelength  $\lambda_i$  ( $\mu\text{m}$ ). We obtained homogeneous observations with the average sensitivity of 1.7 Jy and the spectral resolution of  $0.04 \text{ km s}^{-1}$  (Szymczak et al. 2000). As one of the aims of this work is to study relationships between methanol and

**Table 1.** Detection rates against flux quality flags at four IRAS bands

flag	band			
	12 $\mu\text{m}$	25 $\mu\text{m}$	60 $\mu\text{m}$	100 $\mu\text{m}$
1	45/262(17%)	23/218(11%)	40/593(7%)	59/688(9%)
2	24/155(15%)	10/151(7%)	21/151(14%)	41/225(18%)
3	107/976(11%)	143/1024(14%)	115/649(18%)	76/480(16%)

infrared sources we discarded a total of 6 masers from our original list of 182 masers, for which there is evidence that they are unrelated to IRAS sources or their methanol spectra are strongly confused by the emission of nearby sources. Specifically, 18447–0229 and 19216+1429 were rejected as their positions are offset by about  $5.5'$ , which is comparable to our antenna beamwidth, from the positions reported by Caswell et al. (1995) and Menten (1991) where much stronger emission was found, whereas 18056–1952, 18056–1954, 18097–1825 and 18443–0231 were rejected because their spectra are badly confused by the methanol emission from a cluster of sources resolved with a smaller antenna beamwidth (Caswell et al. 1995).

### 3. Detection statistics

#### 3.1. Qualities of infrared flux density measurements

IRAS measurements of flux densities were made with different qualities. The measurements of good and moderate qualities are assigned by flags 3 and 2 respectively and the upper limits are flagged by 1 (IRAS Explanatory Supplement 1985).

Detection rates of methanol sources against quality flags at four IRAS bands are given in Table 1. Among sources with flag 3 the detection rate increases from 11% at 12  $\mu\text{m}$  to 18% at 60  $\mu\text{m}$  and slightly decreases at 100  $\mu\text{m}$ . Much steeper increase of the detection rate is seen for sources with flag 2 in the band range from 25  $\mu\text{m}$  to 100  $\mu\text{m}$ , while it is 16% at 12  $\mu\text{m}$ . An opposite tendency is evident for sources flagged by 1; the detection rate decreases from 17% at 12  $\mu\text{m}$  to 7% and 9% at 60  $\mu\text{m}$  and 100  $\mu\text{m}$  respectively. This may suggest that at longer wavelengths the intrinsic flux densities are much weaker than given by upper limits, if the methanol masers are pumped by the far-infrared photons.

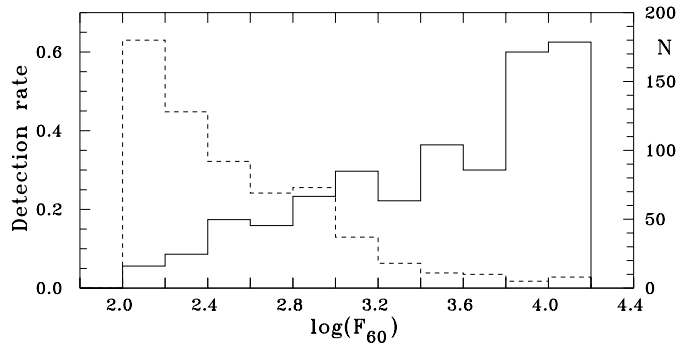
Relative increase of the number of new masers depending on quality flags at IRAS bands is given in Table 2. Among the objects with flags 3 and 2 about 33% and 37% of masers respectively are new sources. Relative increase of maser sources in objects with flag 1 at 25  $\mu\text{m}$ , 60  $\mu\text{m}$  and 100  $\mu\text{m}$  bands is nearly 60%. This proves usefulness of our strategy to search for maser emission in the sample unbiased by restrictions imposed on the infrared measurement qualities.

#### 3.2. IRAS flux density

95 sources altogether from the subsample of 631 IRAS objects with good or moderate measurement qualities at 12, 25 and 60  $\mu\text{m}$  bands, drawn from the original sample, are associated with methanol masers. The detection rate as a function of the

**Table 2.** Relative increase of new masers against flux quality flags at four IRAS bands

flag	band			
	12 $\mu\text{m}$	25 $\mu\text{m}$	60 $\mu\text{m}$	100 $\mu\text{m}$
1	22/45(49%)	14/23(61%)	23/40(57%)	34/59(58%)
2	9/24(37%)	3/10(30%)	9/21(43%)	15/41(37%)
3	39/107(36%)	53/143(37%)	38/115(33%)	21/76(28%)

**Fig. 1.** Detection rate of the 6.7 GHz masers versus the 60  $\mu\text{m}$  flux density (solid line). The total number of sources ( $N$ ) in each bin is shown by dashed line.

IRAS 60  $\mu\text{m}$  flux density for this subset is shown in Fig. 1. The probability to detect the methanol emission is about 62% for sources with 60  $\mu\text{m}$  flux density of above  $10^4$  Jy, then steadily decreases for weaker sources. Only 7% of objects with the flux density in the range from 100 to 250 Jy are methanol sources. A similar trend is kept for 12  $\mu\text{m}$  and 25  $\mu\text{m}$  bands. Fig. 1 indicates that similarly to OH masers (Cohen et al. 1988), the methanol detections are found among luminous IRAS sources. We expect that with the present sensitivity further observations of sources with  $F_{60} < 100$  Jy would not produce a significant number of new masers. This appears to be consistent with the result obtained by van der Walt et al. (1996), who found 5 masers out of 241 southern colour-selected IRAS sources with  $F_{60} < 100$  Jy. Their detection rate of about 2% was about three times lower than our rate for sources with  $100 < F_{60} < 125$  Jy, partly due to their lower sensitivity.

#### 3.3. Galactic location

The distribution of the detection rate of methanol masers versus galactic longitude is shown in Fig. 2. The rate was calculated for the whole sample as the ratio of the number of masers to the total number of searched objects per  $10^\circ$  longitude bin. As our survey is complete for sources with  $\delta > -20^\circ$ , the first and last longitude bins in Fig. 2 are slightly underpopulated. In the longitude range  $10$ – $50^\circ$  the detection rate is about 18% and drops to about 5% for  $70 < l < 90^\circ$  and  $100 < l < 120^\circ$ . With the exception of the latter interval the anticentre region  $90 < l < 240^\circ$  is poorly populated by methanol sources. A high detection rate for galactic longitudes of about  $130^\circ$  and  $180^\circ$  (Fig. 2) is due to the statistics of small numbers; the number of studied

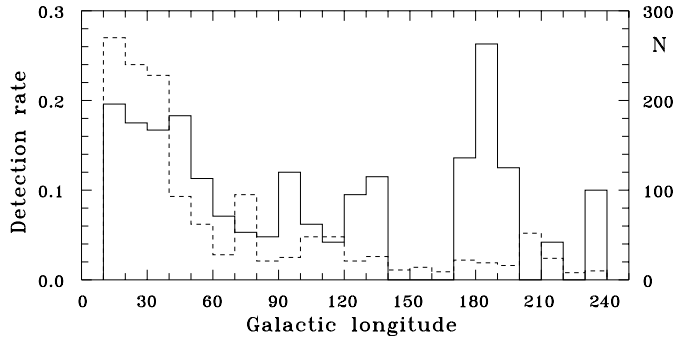


**Fig. 2.** Detection rate of the 6.7 GHz masers versus the galactic longitude (solid line). The total number of sources ( $N$ ) in each bin is shown by dashed line.

objects in each bin is commonly lower than 25. We estimated that for the longitude range 120–240° the mean detection rate is 2.3%. Therefore, the probability to detect the methanol emission in the inner galactic region is about a factor of 8 higher than that in the outer Galaxy. Previous studies of methanol source distribution in the Galaxy established a similar general trend (van der Walt et al. 1995), but quantitative results based on smaller and inhomogeneous sample (Slysh et al. 1999) are quite different from ours.

84% (122/147) of methanol masers with  $l \leq 70^\circ$  lie within  $|b| < 0.5^\circ$ . The mean detection rate for this galactic latitude range is 18%. High galactic longitude sources ( $l > 70^\circ$ ) have a flat distribution in the galactic latitude range from  $-6.3$  to  $5.5^\circ$ . Only one source 06053–0622 (Mon R2) has  $b = -12.6^\circ$ . We confirm the finding by van der Walt et al. (1995) that the galactic distribution of the 6.7 GHz methanol masers closely follows the distribution of molecular gas seen in the CO line (Dame et al. 1987).

## 4. Line properties

### 4.1. Linewidth

A Gaussian component analysis of each methanol spectrum of all the 176 sources was performed. A total of 1354 components were identified and the flux density and the full width at half maximum (FWHM) were measured. The lower panel of Fig. 3 shows the distribution of FWHM of Gaussian components. The mean FWHM of methanol feature is  $0.17 \text{ km s}^{-1}$  and the median value is  $0.14 \text{ km s}^{-1}$ . We identified well separated features of FWHM of about  $0.10 \text{ km s}^{-1}$ . Menten (1991) reported the narrow unblended components of widths  $0.3$ – $0.5 \text{ km s}^{-1}$ . Typical narrow features having the FWHM of  $0.25 \text{ km s}^{-1}$  were found by Caswell et al. (1995). The lowering of the average FWHM found in our study is mainly due to the detection of several faint sources with very narrow features. Fig. 3 suggests that there is a lower limit of  $0.05 \text{ km s}^{-1}$  to the linewidths of individual components in the 6.7 GHz maser spectra.

The plot of the flux density fitted for each component against its FWHM is shown in the upper panel of Fig. 3. For narrow features with the  $\text{FWHM} < 0.10 \text{ km s}^{-1}$  we see an increase of the

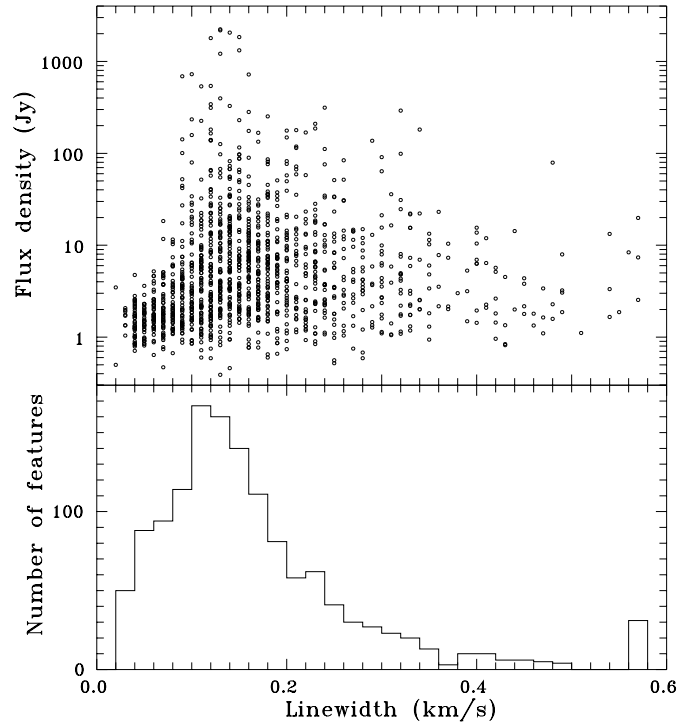


**Fig. 3.** The fitted flux densities of maser components versus the linewidths (upper panel). Distribution of the linewidth, FWHM (lower panel). The cumulative number of sources with  $\text{FWHM} > 0.5 \text{ km s}^{-1}$  is shown in the last bin.

flux density with the linewidth. In the FWHM range from  $0.10$  to  $0.20 \text{ km s}^{-1}$ , the flux densities differ by more than 3 orders of magnitude. A gradual decrease of the flux density occurs for the FWHM higher than  $0.14 \text{ km s}^{-1}$ . Almost all the features with the FWHM greater than  $0.35 \text{ km s}^{-1}$  have the flux densities lower than  $10 \text{ Jy}$ . We identified faint broad features for which the FWHM estimates are certain, but we cannot exclude the possibility that some of them are blended, so that the Gaussian analysis could be less reliable. Despite some possible minor errors of our Gaussian analysis the relation between the flux density and the linewidth may reflect intrinsic properties such as maser gains and/or kinetic temperatures in maser regions. This relation will be discussed further within the framework of the standard maser theory.

### 4.2. Maser velocity range

The velocity range of methanol emission ( $\Delta V$ ) varies from  $0.5$  to  $18.2 \text{ km s}^{-1}$  for sources 18196–1331 and 18438–0222 respectively. There are sources with a single narrow feature of FWHM of about  $0.10 \text{ km s}^{-1}$  and sources with complex spectra composed of several well separated and/or blended features. A large diversity of methanol maser spectra was discussed by Caswell et al. (1995) and we notice that most of their general comments are applicable to our data. Here, we confine ourselves only to present the distributions of the maser velocity range in two subsets of our sources (Fig. 4) distinguished by the average linewidth ( $\langle \text{FWHM} \rangle$ ), which is the arithmetic mean of FWHM of

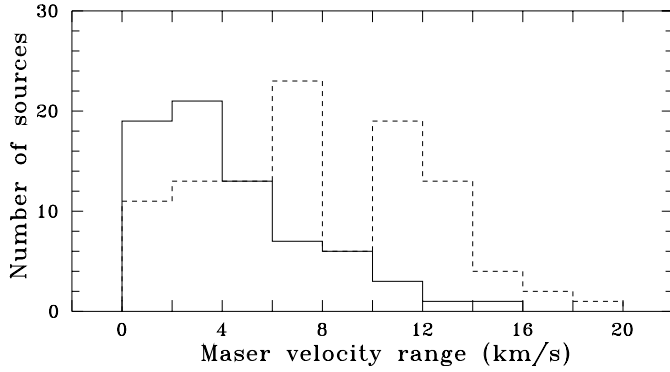


**Fig. 4.** Distributions of the velocity range of maser emission in sources with  $\langle \text{FWHM} \rangle \leq 0.14 \text{ km s}^{-1}$  (solid line) and  $\langle \text{FWHM} \rangle > 0.14 \text{ km s}^{-1}$  (dashed line).

all the Gaussian components distinguished in the source spectrum. In the subsample with  $\langle \text{FWHM} \rangle \leq 0.14 \text{ km s}^{-1}$ , most of the sources have  $\Delta V < 6 \text{ km s}^{-1}$ . The distribution of  $\Delta V$  in the sources with  $\langle \text{FWHM} \rangle > 0.14 \text{ km s}^{-1}$  is flat with only a slight excess of sources with a large maser velocity range. To assess the significance of the differences between these distributions we used the Kolmogorov-Smirnov (K-S) test. The probability that both the subsamples have the same distributions of  $\Delta V$  is lower than  $10^{-4}$ . This substantial difference may be a simple consequence of different evolutionary stages of both groups.

## 5. Masers and infrared properties

### 5.1. Colour-colour diagram

Fig. 5a shows the IRAS two-colour diagram for all the methanol detections. The colour  $[\lambda_i - \lambda_j]$  is defined as  $\log(F_{\lambda_i}/F_{\lambda_j})$ . The sources with upper limits at one or more IRAS bands are marked by crossed symbols and they are not discussed in the following. In our sample there are 95 sources with well determined colours. 17 of them, including 13 new sources, lie outside the colour limits established for UCHII regions by Wood & Churchwell (1989) (hereafter WC89). The  $[25-12]$  colours of 5 sources are even bluer than those expected for IRAS sources satisfying less stringent criteria for UCHII regions (Hughes & MacLeod 1989, hereafter HM89). Further inspection revealed that the sources in the upper left corner of the diagram are relatively weak masers with small  $\Delta V$ .

Fig. 5b shows colour-colour diagram for all the sources with IRAS flags 3 or 2 at 12, 25 and  $60 \mu\text{m}$  undetected in the methanol line, together with the detection rate superimposed. At first look the success rate to detect masers is the largest for the reddest sources. This trend noticed in the previous study possibly reflects an evolutionary track of massive stars from cold dark clouds to objects with UCHII regions of increasing angular extent (MacLeod et al. 1998). However, we must note that the estimates of detection rates in the sources with the extreme red colours are much less reliable than in the sources with bluer colours. In all the bins with the detection rate equals to the unity only one object was observed. When we consider only the

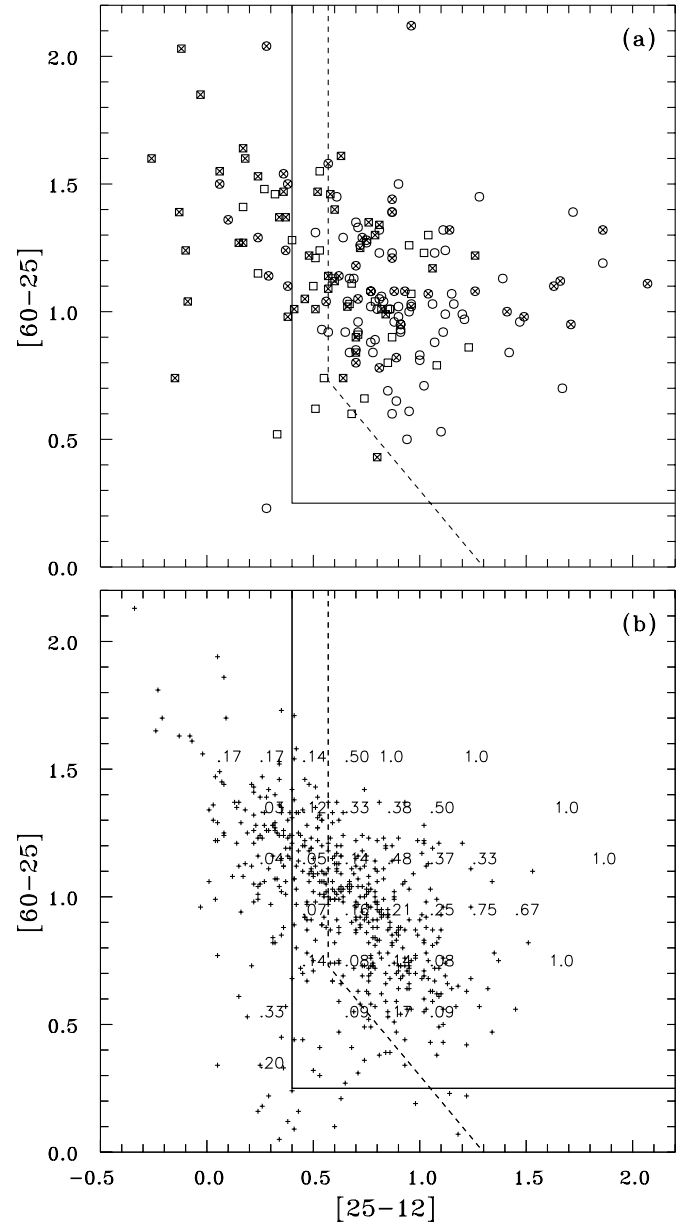


**Fig. 5a and b.** The IRAS colour-colour diagrams for all the maser sources **a** and for non-detections **b**. The newly detected sources are indicated by circles and the known sources are indicated by squares. The crossed symbols indicate the sources with upper limits at one or more IRAS bands, so that their colours are either upper, lower limits, or are undetermined. Dashed and solid lines delineate the WC89 and HM89 criteria for UCHII regions respectively.

central high-density part of the diagram, where the number of sources is higher than 10 in each 0.2 by 0.2 bin, it is clear that the highest detection rates are for intermediate colours. The maximum detection rate is near  $0.8 < [25-12] < 1.0$  for  $[60-25] < 0.8$ , then with increase of  $[60-25]$  the maximum shifts towards redder  $[25-12]$  colours. We notice the same trend for high-density parts of the colour-colour diagram published by van der Walt et al. (1995). This strongly suggests that the maser favouring conditions appear in objects of specific colours.

It is remarkable that in the high-density part of the diagram near about  $[25 - 12] \cong 0.5$  and  $[60 - 25] \cong 1.1$  the detection rate is usually lower than 5% for the 0.2 by 0.2 bins. However, in two extreme, above mentioned, parts of the diagram populated by weak masers with small  $\Delta V$ , the detection rates being commonly higher than 15% do not follow a smooth decreasing trend towards blue colours. These relatively high rates are possibly due to the low number of the objects studied. The presence of masers outside the UCHII region of the two colour diagram defined by WC89 criteria suggests that those criteria are too stringent to identify all the UCHII regions. Indeed, our inspection of the UCHII region catalogue (Becker et al. 1994) revealed that at least the maser source 18441-0134 has a counterpart at 5 GHz. Alternatively, it is possible that there are massive stars with the methanol emission that have indices differing from those of a typical UCHII region. This view may be supported by blind observations of a narrow strip of the galactic plane that resulted in discovery of a small group of masers with very blue IRAS colours (Ellingsen et al. 1996).

### 5.2. $\Delta V$ and IRAS colour

In our sample 115 sources have well determined  $[25-12]$  colour. They were divided into three groups depending on the  $\Delta V$  value. The distributions of the colour in each group are shown in Fig. 6. There is a clear evidence that the median colours increase with the velocity range of methanol emission. Among the bluest sources there are not masers with high  $\Delta V > 8.0 \text{ km s}^{-1}$ . Statistically significant difference at a level less than  $10^{-2}$  (K-S test) is between the sources with  $\Delta V \leq 4.0 \text{ km s}^{-1}$  and  $\Delta V > 8.0 \text{ km s}^{-1}$ . Because the IRAS colours are possibly related to the evolution of methanol sources (MacLeod et al. 1998), the trend seen in Fig. 6 suggests that in statistical sense, the velocity range of emission decreases for most evolved objects. We suspect that at the end of the evolutionary phase with the methanol sources, the maser intensity drops, so that only the brightest features are visible and maser conditions can be sustained only in a few clouds of similar radial velocities.

### 5.3. Maser and infrared flux densities

Fig. 7 shows the 6.7 GHz peak flux density as a function of the  $60 \mu\text{m}$  flux density for 136 sources of IRAS flag 3 or 2. The  $60 \mu\text{m}$  flux densities are always less than the 6.7 GHz maser flux densities. The correlation coefficient for the data is 0.47. This indicates that both the quantities are only weakly correlated. We achieved no significant improvement of the correlation when the integrated maser flux densities were considered. Although our result generally confirms previous studies where little or no correlation between the methanol maser flux density and IRAS flux density was found (van der Walt et al. 1995; Walsh et al. 1997), it is interesting to note that our correlation coefficient is about 2.6 times higher than that reported by van der Walt et al. (1995). The improvement of the correlation coefficient in our study can be due to the observations of less dense parts of the Galaxy, so that confusion may affect our data less than those

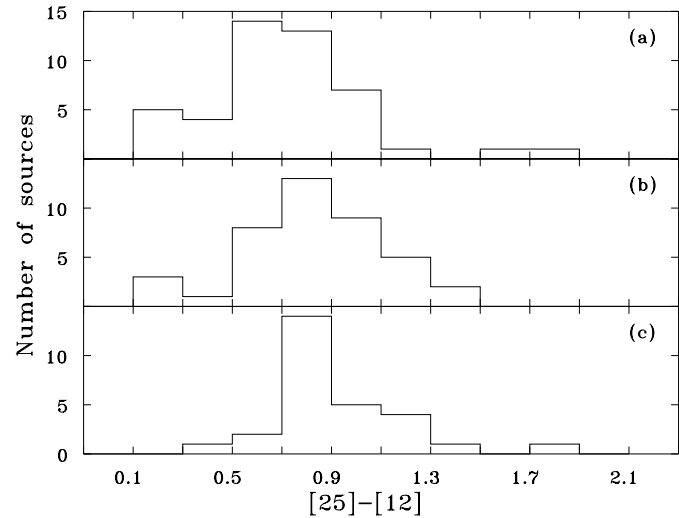


**Fig. 6a-c.** Distributions of IRAS colour in three groups of methanol sources with different velocity ranges of maser emission ( $\Delta V$ ). **a**  $\Delta V \leq 4.0 \text{ km s}^{-1}$ , **b**  $4.0 < \Delta V \leq 8.0 \text{ km s}^{-1}$ , **c**  $\Delta V > 8.0 \text{ km s}^{-1}$ .

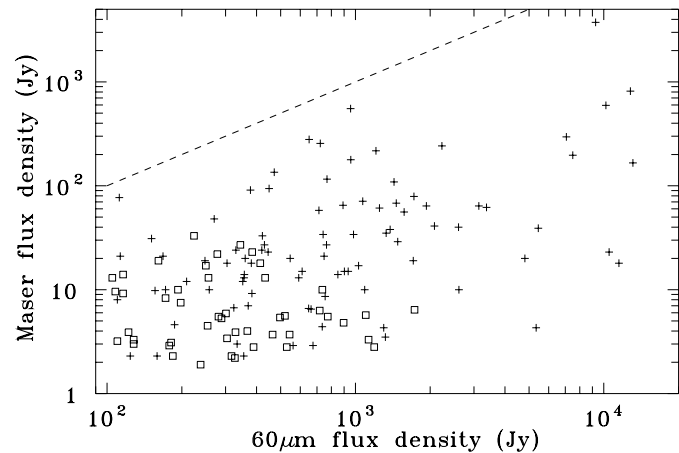


**Fig. 7.** The 6.7 GHz maser peak flux density versus the  $60 \mu\text{m}$  flux density. The newly detected sources are marked by squares and the known sources by crosses. The dashed line represents the case when the maser and  $60 \mu\text{m}$  flux densities are equal.

obtained by the above cited authors, who observed the southern hemisphere sources including the galactic centre. We suggest that the far-infrared radiation cannot be excluded as a possible pumping agent. When infrared photons are converted into maser emission, the median value of the maser to  $60 \mu\text{m}$  photon ratio within our sample is about 0.03. It is very close to the value found for interstellar OH masers (Cohen et al. 1988).

## 6. Discussion

### 6.1. Maser luminosity

To study the intrinsic properties of maser sources we computed the kinematic distances from the central velocities of the methanol spectra using the galactic rotation curve of Brand & Blitz (1993). The largest errors in this method are due to the am-

biguity between near and far distances. To resolve this problem we have applied the approach used by Walsh et al. (1997). In general, we adopted the near kinematic distances for about 80% of the sources. When the near kinematic distance implied a luminosity of maser much weaker than that expected for an UCHII region, we assumed the far kinematic distance. In other ambiguous cases we used the distance estimates obtained by methods other than based upon the systemic velocities and galactic rotation model. We found out that 34 methanol sources in our own sample and the Walsh's et al. (1997) sample are common. Their distance estimates for sources with distance  $\leq 7$  kpc differ by less than 20% from ours. However, for more distant objects the agreement is much worse.

Assuming that the maser emission is isotropic we derived the following formula for the methanol maser luminosity  $L_m$  (photons  $s^{-1}$ ),

$$L_m = 6.0 \cdot 10^{41} D^2 S_i \quad (1)$$

where  $S_i$  is the integrated flux densities in  $Jy km s^{-1}$  and  $D$  is the distance in kpc. The maser photon luminosity of the sources in our sample ranges from  $9 \cdot 10^{40}$  to  $1 \cdot 10^{46} s^{-1}$  (Fig. 8) and the median value is  $6 \cdot 10^{43} s^{-1}$ . Nearly all the sources have  $3 \cdot 10^{42} < L_m < 1 \cdot 10^{45} s^{-1}$ . The lower limit is partly due to the observational selection effect. Our  $3\sigma$  detection limit of  $1.7 Jy$  corresponds to the upper limit in the integrated flux level of about  $2 \cdot 10^{-22} W m^{-2}$ . Thus, for the sources with the intrinsic luminosity greater than  $3 \cdot 10^{42} s^{-1}$  we have completeness to the distance of 2.2 kpc. The median luminosity in this solar neighbourhood is  $2 \cdot 10^{43} s^{-1}$  and does not depend on the galactic longitude. Palla et al. (1991) observed the  $H_2O$  22 GHz maser emission in a sample of dense clouds possibly at the very earliest stages of star formation. The water maser luminosity averaged for these nearby sources ( $D < 2.2$  kpc) is one order of magnitude higher than the above estimated methanol maser luminosity. Caswell et al. (1995) claimed that the 6.7 GHz methanol maser intensities are typically 7 times higher than the 1.6 GHz OH maser intensities.

There are seven brightest sources with luminosities higher than  $3 \cdot 10^{45} s^{-1}$ . W3OH (02232+6138) is probably the brightest source in our sample, its luminosity is  $8 \cdot 10^{45} s^{-1}$  at the near kinematic distance of 1.3 kpc, but it would be about  $2 \cdot 10^{46} s^{-1}$  for commonly accepted distance of 2.2 kpc (Humphreys 1978). The luminosity of the brightest methanol source whenever observed 9.62+0.20 (Caswell et al. 1995) is probably about one order of magnitude higher than that of W3OH.

## 6.2. The gas kinetic temperature

The analysis done in Sect. 5.1 suggests that there is a lower limit to the linewidths of individual components of the methanol spectra. It is generally accepted that the profile of a maser line is approximately Gaussian and, following the classical theory (Goldreich & Kwan 1974), has a linewidth

$$\Delta\nu \approx \Delta\nu_D / \sqrt{-\tau} \quad (2)$$

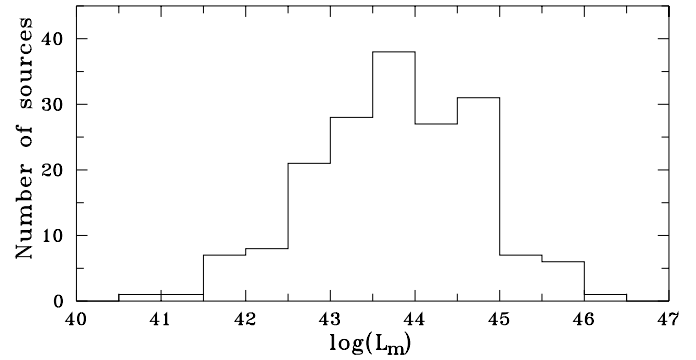


Fig. 8. Distribution of the photon luminosities ( $L_m$ ) of the all the 176 analyzed methanol maser sources.

for unsaturated amplification. Here  $\Delta\nu_D$  is the thermal (Doppler) linewidth and  $\tau$  is the optical depth of the negative value. The maser intensity increases by a factor of  $e^{-\tau}$  and the linewidth decreases until the centre of the maser line starts to saturate. The typical brightness temperature of methanol masers of  $1.4 \cdot 10^{11} K$  (Menten et al. 1992; Sobolev et al. 1997) implies  $\tau = -25.7$ . Thus, the methanol line will narrow  $\sqrt{25.7}$  times, so that the minimum linewidth of about  $0.05 km s^{-1}$  will appear for the thermal linewidth of  $0.25 km s^{-1}$ . This linewidth for the methanol molecule implies the kinetic temperature of 35 K, which agrees very well with that applied in the standard methanol maser model by Sobolev et al. (1997). However, when the maser emission in the line centre becomes saturated its intensity increases more slowly (linearly) than intensities in the line wings and the linewidth approaches to be equal to the thermal width again. Although the degree of saturation of an individual maser component is unknown, the observational fact that nearly 90% of the maser components identified have  $FWHM < 0.25 km s^{-1}$ , can imply that the kinetic temperature is not higher than 35 K in most sources.

The initial increase of the fitted flux density with the linewidth seen in Fig. 3 does not rule out the above interpretation of the maser line narrowing. It can be easily explained as the cause of the selection effect. The most distant sources should be stronger, to be observed with a given sensitivity, than the relatively nearby sources. Relation (2) discussed above implies that the intrinsically strong components are more affected by the line narrowing than the weaker ones. In consequence, the observed flux densities increase with the linewidths.

91 objects in our sample were detected in the ammonia lines by Molinari et al. (1996) and 22 of them are methanol sources. The ammonia lines are commonly recognized as important signposts of the primordial stages of massive star formation. If they come from the same or adjacent regions as methanol masers, an independent estimate of the gas kinetic temperature can be obtained. We found that the mean  $T_k$  for the ammonia sources with the methanol emission is 27 K. This value is quite close to our upper limit for  $T_k \cong 35 K$  inferred above from the methanol maser linewidth. A detailed study of the relations between the methanol and ammonia lines is needed to prove this.

### 6.3. Evolutionary implications

A suggestion for evolution of massive star-forming regions associated with the methanol masers is based on the differences in the detection rates between the blue and red sources (MacLeod et al. 1998). They suggest that the reddest IRAS sources are the youngest. Our data do not confirm a smooth decreasing trend in the detection rate from the reddest sources to the bluest ones. Instead, we found that the maximum detection rate of the methanol masers occurs for objects of specific range of colours. Our finding is consistent with the results based mostly on the southern sources (van der Walt et al. 1995). The present study also provides further evidence of possible evolutionary changes of maser properties. First of all we found significant differences in the distributions of  $\Delta V$  of the two subsets of sources of low and high linewidths. More specifically, a substantial fraction of sources with low and high  $\Delta V$  have features of high  $\langle \text{FWHM} \rangle$ , but low  $\Delta V$  sources have usually low  $\langle \text{FWHM} \rangle$ . Furthermore, we also found that the median [25 – 12] colour increases with  $\Delta V$  and in the bluest sources  $\Delta V$  is commonly lower than  $8.0 \text{ km s}^{-1}$ . It is likely that in an earlier stage the methanol emission emerges from only a few clouds of low kinetic temperature, surrounding a massive star without or ongoing forming UCHII region characterized by the reddest IRAS colours; we observe narrow lines within narrow velocity range. When an UCHII region is already formed and begins to disperse circumstellar matter, more clouds of different radial velocities and higher  $T_k$  sustain maser emission, thus the observed  $\Delta V$  and  $\langle \text{FWHM} \rangle$  and the detection rate increase. Further increase of  $T_k$  and size of an UCHII region results in quenching of maser emission in most clouds or even in the whole source;  $\Delta V$  decreases but the linewidth is high and the colours are blue.

Our hypothesis assumes that the methanol emission primarily comes from clumps. The clump hypothesis of the origin of methanol maser sources was proposed by Sobolev & Deguchi (1994). They suggested that isolated elongated clumps of methanol masers are influenced by the shock waves. It is still unclear whether those clumps are formed by interaction of the shock with the interstellar cloud or they are primordial clouds. However, the shock may align the clumps into organized structures (Sobolev et al. 1997). Our hypothesis of methanol maser evolution appears not to be in conflict with the origin of the methanol emission from a protostellar disc (Norris et al. 1993) where the maser sources are represented by regions of correlated velocities or clumps. A weak point of our hypothesis is that the linewidth of an individual maser component or  $\langle \text{FWHM} \rangle$  in a maser source is a simple function of the gas kinetic temperature. Only for a given maser gain, the linewidth of an individual feature is primarily determined by  $T_k$ . It is difficult to expect that the maser gain and the degree of saturation do not change from source to source. The observations with sub-arcsec resolutions to measure the basic properties of individual maser spots and their structures and kinematics will be very instructive to examine our hypothesis. What is more, studies of temporal changes of selected sources can provide data on the degree of saturation.

### 7. Conclusions

We have analyzed the results of comprehensive survey of the 6.7 GHz maser line in a sample of IRAS selected regions of star formation.

The detection rate strongly depends on the galactic location and the far-infrared flux densities but weakly depends on the qualities of IRAS flux density measurements.

The distributions of the maser velocity range, the mean linewidth and the detection rate reflect evolutionary changes of methanol sources.

There are new maser sources with colours outside the colour ranges of typical ultracompact HII regions. They deserve particular attention in future studies.

The gas kinetic temperature of less than 35 K in the methanol regions was inferred from the lower limit observed for the linewidth.

A weak correlation of the maser flux density with the far-infrared flux density does not exclude a possible pumping mechanism by infrared photons with an efficiency comparable to that for interstellar OH masers.

*Acknowledgements.* This work was supported by the Polish State Committee for Scientific Research through grant 2P03D01415.

### References

- Becker R.H., White R.L., Helfand D.J., Zoonematkermani S., 1994, *ApJS* 91, 347
- Brand J., Blitz L., 1993, *A&A* 275, 67
- Caswell J.L., 1996, *MNRAS* 279, 79
- Caswell J.L., Vaile R.A., Ellingsen S.P., Whiteoak J.B., Norris R.P., 1995, *MNRAS* 272, 96
- Cohen R.J., Baart E.E., Jonas J.L., 1988, *MNRAS* 231, 205
- Dame T.M., Ungerechts H., Cohen R.S., et al., 1987, *ApJ* 322, 706
- Ellingsen S.P., von Bibra M.L., McCulloch P.M., et al., 1996, *MNRAS* 280, 378
- Goldreich P., Kwan J., 1974, *ApJ* 190, 27
- Hughes V.A., MacLeod G.C., 1989, *AJ* 97, 786
- Humphreys, R. M., 1978, *ApJS* 38, 309
- IRAS Explanatory Supplement, 1985, Joint IRAS Science Working Group, eds. C.A. Beichman et al., U.S. Government Printing Office, Washington DC
- IRAS Point Source Catalog, 1985, IRAS Science Working Group, U.S. Government Printing Office, Washington DC
- MacLeod G.C., Gaylard M.J., 1992, *MNRAS* 256, 519
- MacLeod G.C., Gaylard M.J., Nicolson G.D., 1992, *MNRAS* 254, 1P
- MacLeod G.C., van der Walt D.J., North A., et al., 1998, *AJ* 116, 2936
- Menten K.M., 1991, *ApJ* 380, L75
- Menten K.M., Reid M.J., Pratap P., Moran J.M., Wilson T.L., 1992, *ApJ* 401, L39
- Molinari S., Brand J., Cesaroni R., Palla F., 1996, *A&A* 308, 573
- Norris R.P., Whiteoak J.B., Caswell J.L., Wieringa M.H., Gough R.G., 1993, *ApJ* 412, 222
- Palla F., Brand J., Cesaroni R., Comoretto G., Felli M., 1991, *A&A* 246, 249
- Schutte A.J., van der Walt D.J., Gaylard M.J., MacLeod G.C., 1993, *MNRAS* 261, 783
- Slysh V.I., Val'ts I.E., Kalenskii S.V., et al., 1999, *A&AS* 134, 115
- Sobolev A.M., Cragg D.M., Godfrey P.D., 1997, *A&A* 324, 211

- Sobolev A.M., Deguchi S., (1994), A&A 291, 569  
Szymczak M., Hrynek G., Kus A.J., 2000, A&AS 143, 269  
van der Walt D.J., Gaylard M.J., MacLeod G.C., 1995, A&AS 110, 81  
van der Walt D.J., Retief S.J.P., Gaylard M.J., MacLeod G.C., 1996,  
MNRAS 282, 1085
- Walsh A.J., Burton M.G., Hyland A.R., Robinson G., 1998, MNRAS  
301, 640  
Walsh A.J., Hyland A.R., Robinson G., Burton M.G., 1997, MNRAS  
291, 261  
Wood D.O.S., Churchwell E., 1989, ApJ 340, 265